Observation of a geometrical resonance effect in $Bi_2Sr_2CaCu_2O_{8+x}$ break junctions

B. A. Aminov, M. A. Hein, G. Müller, H. Piel, and D. Wehler
Fachbereich Physik, Universität Wuppertal, 42097 Wuppertal, Germany

V. Z. Kresin
Lawrence Berkeley Laboratory, University of California at Berkeley, Berkeley, California 94720

Ya. G. Ponomarev
Physics Faculty, Moscow State University, 119899 Moscow, Russia

L. Buschmann, L. Winkeler, and G. Güntherodt
2. Physikalisches Institut, Rheinisch-Westfälische Technische Hochschule Aachen, Aachen, Germany
(Received 11 March 1996)

A periodic structure has been observed in the tunneling characteristics of $Bi_2Sr_2CaCu_2O_{8+x}$ break junctions. The observed structure is explained by the electron-hole interference effect in the surface layer, which produces a periodic structure in the tunneling characteristics. Good qualitative agreement has been obtained between measured data and calculated with Arnold's proximity model characteristics. The observed effect indicates an important role of the proximity effect on surface sensitive properties of high-T_c superconductors, and explains the reported discrepancy of energy-gap values for $Bi_2Sr_2CaCu_2O_{8+x}$. [S0163-1829(96)02033-4]

INTRODUCTION

Since the discovery of high-T_c superconductors (HTSC's) many attempts have been made to obtain information about the energy spectra of these materials. Traditionally, tunneling spectroscopy is one of the most powerful tools for solving this problem.[1] However, many tunneling experiments realized with different techniques gave controversial results [for a review see Ref. 2]. In particular, a wide range of energy-gap values $0 \leqslant 2\Delta/kT_c \leqslant 12$ has been reported both for $YBa_2Cu_3O_{7-x}$ (YBaCuO) and for $Bi_2Sr_2CaCu_2O_{8+x}$ (BiSrCaCuO) HTSC's.

As will be shown below, one possible reason for this large spread is a spatial inhomogeneity of HTSC's near the surface. The very short coherence length in HTSC's, which is of the order of magnitude of the unit cell, leads to a reduced pair potential at surfaces and to the formation of a surface layer with reduced superconducting properties.[3] In addition, a natural Schottky-type barrier can form at the surface, modifying the surface range.[4] Finally, poor surface properties and defects are expected from atmospheric surface degradation of HTSC's and/or reaction/diffusion between the HTSC and the barrier layer in artificial junctions. The formation of such a complex surface structure requires to consider the proximity effect, which would be directly reflected on the tunneling characteristics, since they are probing the electronic properties at the surface.

In this paper we report observation of $I(V)$ characteristics of $Bi_2Sr_2CaCu_2O_{8+x}$ break junctions with current steps, and, consequently, a sharp structure in the conductance-voltage characteristics. The observation of such features indicates on the formation of a complex $S/N-I$ structure (S is for superconductor, N is for normal metal, and I is for insulator) at the surface, and the presence of bound states in the excitation spectrum of the N layer.

First, the proximity effect was considered to explain the tunneling spectra of $Bi_2Sr_2CaCu_2O_{8+x}$ (Ref. 5) based on the McMillan ''tunneling'' proximity model with weakly coupled N and S layers and the coherence length ξ_N comparable to the thickness of the normal surface layer $d_N (d_N \approx \xi_N)$.[6] Here, we have used the limit of strongly coupled N and S layers with $d_N \geqslant \xi_N$ and $l \geqslant d_N$ (l is the mean free path).[7] In this case the electron-hole interference effect becomes important, which essentially modifies the local density of states (DOS) at the interface between normal and insulating layers.[8] In particular, for relatively large values of d_N equally spaced bound states appear in the superconducting energy gap, which produce current steps in $I(U)$ and a peaked structure in $dI(U)/dU$ characteristics.

EXPERIMENTAL

The details of the $Bi_2Sr_2CaCu_2O_{8+x}$ single-crystal preparation were described in Ref. 9. The presented data are based on the measurements of the more than 50 ''as-grown'' single crystals, split from one large matrix with many thin crystals attached to it.

Tunnel junctions were formed as the result of a mechanical contact between two cryogenic fracture surfaces (break junctions).[10] The current and potential contacts to the four corners of the rectangular crystals were prepared from fresh indium-gallium solder, which is liquid at room temperature. This prevented the crystals from being damaged. The crystals were mounted on a working platform made of copper foil-coated fiberglass with a stress concentrator (a groove) in the central part of the platform. The platform itself was glued to a beryllium bronze spring. A crack in the crystals was produced at liquid-helium temperature by deforming the platform which a micrometer screw. Before being placed in the cryostat, the platform was slightly deformed. As a result,

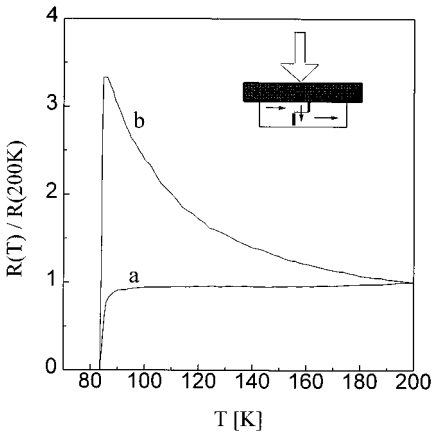

FIG. 1. Typical temperature dependences of the resistance along ab (a) and c directions (b) of the $Bi_2Sr_2CaCu_2O_{8+x}$ single crystals. The inset shows the method of the break-junction preparation with the steplike shape of the crack.

after cool down, it was possible not only to produce a crack in the crystal but also to release it. It should be noted that the break-junction technique allows one to investigate the uncontaminated surface properties of materials.

Before the crack formation, the temperature dependence of the sample resistance was measured. The zero resistance temperature of the uncleaved samples was highly reproducible in the range 82–83 K with a transition width of 1–2 K (Fig. 1). A computer-controlled bridge compensation circuit was used for recording $I(U)$, $dI(U)/dU$, and $d^2I(U)/dU^2$ characteristics. The formation of a crack was controlled by observing the changes of $I(U)$ characteristics on the computer monitor.

RESULTS AND DISCUSSIONS

In Fig. 2(a) several $I(U)$ characteristics are shown for different break junctions, produced with the same single crystal by a slight variation of the bending screw. The characteristics reveal a structure with a different number of current steps at different voltages. The current steps on $I(U)$ curves correspond to a peaked structure in the conductance-voltage characteristics as shown in Fig. 2(b). The number and the periodicity of the peaks in the $dI(U)/dU$ characteristics vary from contact to contact, but with general behavior: the largest number of peaks occurs with the smallest period and with the first peak at the lowest voltages. As the first peak shifts to higher voltages the distance between the peaks increases, and the number of the peaks decreases, until only one conductance peak can be observed [Fig. 2(b)].

The observed characteristics are essentially different from the tunneling spectra of a homogeneous S-I-S junction structure (S is for superconductor and I is for insulator).[1] The periodic structure has been observed before in the tunneling characteristics of high-T_c superconductors using scanning tunneling microscopy (STM).[11] The explanation, which has been proposed in terms of the charging effect, assumes the formation of S-I-$S'(N')$-I-N junctions with ultrasmall junction areas (typically 10^{-5}–10^{-4} μm^2). $S'(N')$ denotes a small superconducting (normal) grain separating the bulk superconducting electrode S and normal conducting scanning

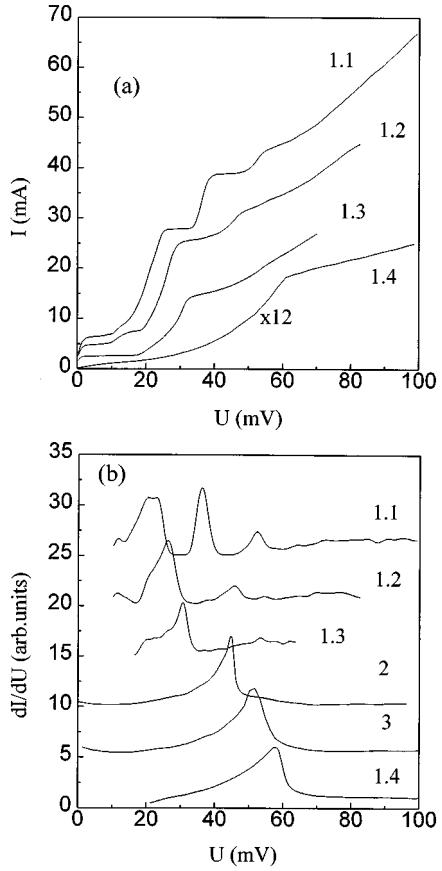

FIG. 2. Current-voltage (a) and conductance-voltage (b) characteristics of different $Bi_2Sr_2CaCu_2O_{8+x}$ ($T_C=83$ K) break junctions at $T=4.2$ K. Characteristics Nos. 1.1–1.4 were observed with the same single crystal.

tip. The current-voltage characteristics of such contacts display equally spaced current steps (Coulomb staircase), when two conditions are satisfied:[12] (1) the charging energy $E_Q=e^2/2C$ is much larger the thermal energy k_BT; (2) the junction resistance R exceeds $R_Q\equiv h/4e^2\approx 6.45$ kΩ. The data in the present publication has been measured on junctions with normal resistance in the range from several Ohms to several hundreds Ohms (see Fig. 2), which is much lower than the quantum resistance value R_Q. It should also be noted, that the voltage period for the Coulomb staircase ΔV_P is determined only by the junction capacitance $\Delta V_P=e/C$, which, in turn, is defined by the geometry of the barrier. Therefore, it is difficult to expect any reproducibility of characteristics, in contrast to what has been found (see below). Thus, the charging-energy effect seems unimportant for our junctions. In order to explain the measured characteristics the formation of a complex S-N-I structure (N denotes the normal metal) at the surface range has been assumed.

As shown on Al-AlO-Cu/Pb by Bellanger *et al.*[13] and on Pb/Zn-I-Pb by Rowell[14] artificial junctions, the presence of a clean normal layer changes essentially the tunneling spectra and leads to the observation of current steps in $I(U)$ characteristics, similar to those observed in our measurements. The current steps are related to the appearance of bound states in the excitation spectrum of the N layer. Bound levels in the potential well, which is formed by the insulating barrier and

the superconducting energy gap, are the result of electron-hole interferences in the N layer, as predicted by de Gennes and Saint-James.[15] The energy and the number of the bound states are determined by the thickness and the electronic properties of the N layer. A finite probability for Andreev reflection at energies $E>\Delta_S$ results in additional geometrical resonances and the formation of virtual bound levels with amplitudes essentially smaller than those of deGennes–Saint-James bound states.[16]

For the formation of the bound state in the considered junction geometry it is necessary that electrons cross the normal layer four times to be twice Andreev and normal reflected. In this case, the resulting resonance energy levels are spaced by $E_{n+1}-E_n \approx h v_F/4d_N$ (Refs. 13–16) (here v_F is the Fermi velocity). With increasing thickness of the N layer, the number of peaks in the conductance-voltage characteristic is expected to increase, and the periods to decrease. In the limit $d_N \to 0$, only the first bound state E_1 is present in the DOS at the energy $E \approx \Delta_S$ (Δ_S is the order parameter in the S layer). Thus, the presence of a N layer at the surface of the break junctions can qualitatively explain the observed characteristics and, in particular, the periodic structure.

In order to extract the important information about the surface properties, the experimental data have been compared with Arnold's proximity model.[8] The model was developed for the case of strongly coupled N-S sandwiches assuming thin, clean N layers, and thick S layers with identical Fermi velocities. Following this model, the tunneling density of states is given in the limit of specular tunneling of electrons with wave vectors normal to the barrier by

$$N_T(E)=\mathrm{Im}\left\{\frac{(E/\Omega_N)[iF(E)\cos(\Delta K^N d_N)+\sin(\Delta K^N d_N)]+i(\Delta_N/\Omega_N)G(E)}{[iF(E)\sin(\Delta K^N d_N)-\cos(\Delta K^N d_N)]}\right\}, \tag{1}$$

$$F(E)=\frac{(E^2-\Delta_S\Delta_N)}{\Omega_S\Omega_N}, \quad G(E)=\frac{E(\Delta_S-\Delta_n)}{\Omega_S\Omega_N}, \quad \Omega_{S,N}=\sqrt{E^2-\Delta_{S,N}^2},$$

$$\Delta K^N d_N=\frac{2Z_N d_N}{\hbar v_F}\Omega_N=R\Omega_N, \quad R=\frac{2Z_N d_N}{\hbar v_F},$$

where E is the energy, Δ_N is the order parameter in the N layer and Z_N is the renormalization coefficient, which is assumed to be $Z_N \approx 1$ (weak-coupling limit). For simplicity scattering effects have been taken into accouont phenomenologically[2] by adding to the energy a finite imaginary part of magnitude:

$$\Gamma=\frac{\hbar v_F}{l}. \tag{2}$$

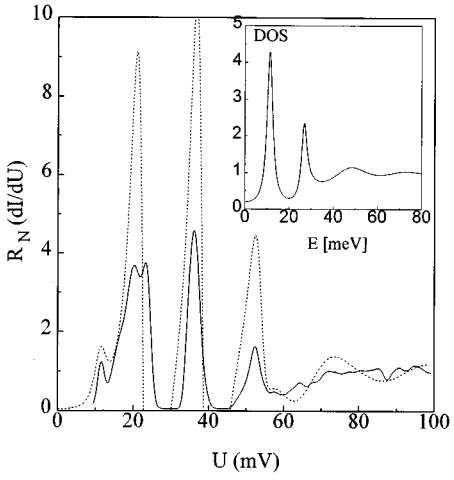

FIG. 3. Conductance-voltage characteristic of a $Bi_2Sr_2CaCu_2O_{8+x}$ ($T_C=83$ K) break junction at $T=4.2$ K (solid line) and the calculation using Arnold's proximity model (dashed line) with the DOS as illustrated in the inset. The fitting parameters are $\Delta_S=28$ meV, $\Delta_N=3$ meV, $R=0.129$ meV^{-1}, and $\Gamma=1.55$ meV.

Using expressions (1) and (2), $I(U)$ and $dI(U)/d(U)$ characteristics have been calculated, assuming symmetric S-N-I-N-S junctions.

Examples of fitting the calculated characteristics to the experimental data are presented in Figs. 3–5. The tunneling density of states used for the calculations is shown in the insets of corresponding figures. The numerical fits show poor quantitative, but very good qualitative agreement between measured and calculated characteristics. In particular, sharp singularities can be well described.

The fits have been obtained by adjusting the four variables Δ_S, Δ_N, R, and Γ, which were taken energy independent for simplicity. The bound-states energies were found to be very sensitive to the first three parameters, whereas the Γ parameter mainly describes the broadening of resonance levels. For the well-defined peak periodicity in the conductance-voltage characteristics, the parameter R can be found separately from the peak interval ΔV_P, $R=2/\Delta V_p$. Then, only two variables remain adjustable. The set of parameters evaluated from the fits are collected in Table I. Remarkable reproducibility can be seen for the energy gap in the S layer.

In terms of the assumed proximity model, the observed characteristic of Fig. 3 corresponds to the case of the thickest N layer with the largest number of bound states. At energies above $2\Delta_S$ peaks corresponding to virtual bound states can be resolved on the calculated characteristic. Such a singularity is not well pronounced on the measured curve (Fig. 3).

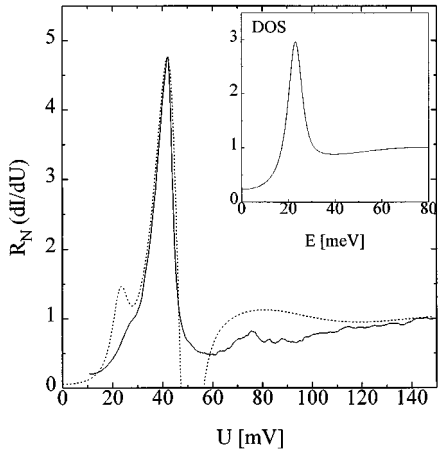

FIG. 4. Conductance-voltage characteristics of a $Bi_2Sr_2CaCu_2O_{8+x}$ ($T_C=83$ K) break junction at $T=4.2$ K (solid line) and the calculation using Arnold's proximity model (dashed line) with the DOS as illustrated in the inset. The fitting parameters are $\Delta_S=29$ meV, $\Delta_N=7$ meV, $R=0.039$ meV^{-1}, and $\Gamma=3.97$ meV.

The discrepancy between data and calculations may be connected with the following reasons. The model assumes the presence of a high insulating barrier $U_B \gg E$, with U_B the height of the insulating barrier. According to the optical microscopy of the cracks performed after the measurements which verified the steplike shape of the cracks as shown in the inset in Fig. 1, the tunneling current was mainly oriented along the c axis. For this direction the formation of the crack in BiSrCaCuO occurs most likely at the BiO planes, where the plane bounding is weakest. From STM (Refs. 17–19) and tunneling[20] measurements it is well known, that the top BiO layer reveals semiconducting properties with half of the energy gap U_B being about 100–200 meV. This value is comparable with the virtual bound-states energies. The low-energy barrier decreases the probability of electrons

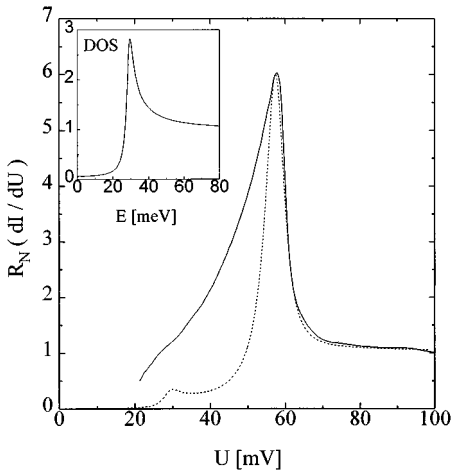

FIG. 5. Conductance-voltage characteristic of a $Bi_2Sr_2CaCu_2O_{8+x}$ ($T_C=83$ K) break junction at $T=4.2$ K (solid line) and the calculation using Arnold's proximity model (dashed line) with the DOS as illustrated in the insert. The fitting parameters are $\Delta_S=29$ meV, $\Delta_N=10$ meV, $R=0.003$ meV^{-1}, and $\Gamma=1.73$ meV.

TABLE I. The set of parameters evaluated from the fits.

E_1 (meV)	Δ_S (meV)	Δ_N (meV)	R (meV^{-1})	d_N (Å)	l (Å)	v_F (10^7 cm/sec)
29	29	10	0.003	3	577	3.30
23.2	29	7	0.039	18	116	1.38
11.4	28	3	0.129	33	165	0.77

reflection and, in turn, reduces the amplitude of the McMillan-Rowell oscillations. The same effect on the amplitude both deGennes–Saint-James and McMillan-Rowell oscillations gives the mismatch of electronic properties, which is not included in the model. Another possible reason may be a reduced mean free path in this energy range due to, for example, phonon emission, when the energy of the electronic excitation is of the order of the phonon energy.[14] Finally, the model assumes a thick S layer with BCS density of states. Since BiSrCaCuO is a quasi-two-dimensional multilayered system, the DOS can be essentially different from the BCS, especially along the c-axis direction.[21–27]

Statistical information on energy E_1 of the first bound state is displayed in Fig. 6. While the range of values is very broad, remarkably well-defined positions can be identified. For junctions of S-N-I-N-S geometry, such a discreteness of E_1 values should be related to the discrete change of the thickness of the N layer. Such a behavior can be understood from the break-junction geometry. As discussed above, the formation of the contact occurs most probably along the c axis with two adjacent split BiO layers acting as a barrier (see Fig. 7). Furthermore, it is well known, that the Cooper pairs are concentrated in the CuO planes. If the double CuO planes, which are closest to the BiO barrier, have the same energy gap as the volume, the superconducting S layer is separated from the barrier by about 6 Å . According to the

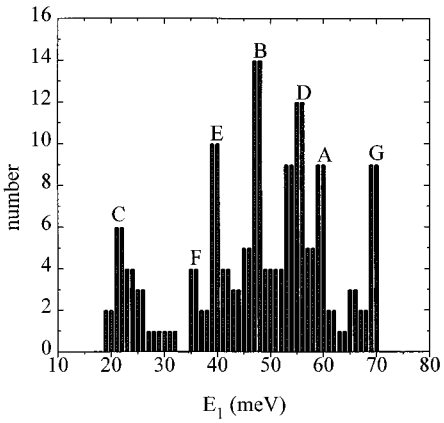

FIG. 6. Histogram of the energies of the first bound state. The peak A with energy $2\times E_{1A}=58.4$ meV corresponds to the contact with geometry S/3 Å/I/3Å -S; peak B corresponds to $2\times E_{1B}=48$ meV (S/18 Å/I/18 Å/S); peak C corresponds to $2\times E_{1C}=20$ meV (S/33 Å/I/33 Å/S); peak D corresponds to $E_{1A}+E_{1B}=53$ meV (S/3 Å/I/18 Å/S); peak E corresponds to $E_{1A}+E_{1C}=39$ meV (S/3 Å/I/33 Å/S); peak F corresponds to $E_{1B}+E_{1C}=34$ meV (S/18 Å/I/33 Å/S). Peak G is interpreted as a result of a contact in the ab plane at the energy $2\times E_{1G}=2\Delta_{ab}=70$ meV.

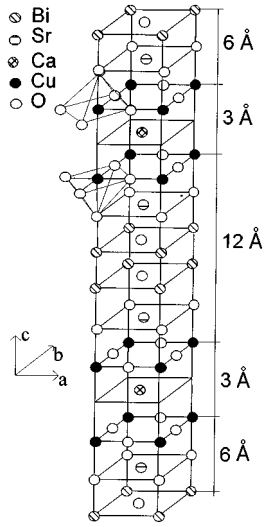

FIG. 7. The crystalline unit cell of $Bi_2Sr_2CaCu_2O_{8+x}$.

crystal structure of Bi-Sr-Ca-Cu-O, only one SrO layer is present between the CuO plane and the BiO layer (Fig. 7), which is expected to act as the *N* layer. Such junctions, in the limit $d_N \rightarrow 0$, correspond to the characteristic presented in Fig. 5. We have approximated this case by the thickness of the *N* layer $d_N = 3$ Å, which is the half the distance from the barrier.

Alternatively, double CuO planes near the barrier could display reduced superconducting properties, and only the next double CuO planes would have the volume energy gap. In this case, the thickness of the *N* layer, with an average energy gap Δ_N, has increased by 15 Å to a total of 18 Å. This procedure can be repeated for the next possible contact geometry, and d_N should increase again by 15 Å. However, if the thickness of the *N* layer will reach the values comparable to the mean free path, then the condition for the clean limit will not be anymore fulfilled, and the interference structure will not be present on the characteristics.

Altogether, the discrete variation of the thickness of the *N* layer is related to the surface BiO layer. The shape and the properties of the barrier strongly depend on oxygen doping. Since the oxygen doping could vary over the fracture surface, which can be expected for ''as-grown'' single crystals, different characteristics are to be observed (Fig. 2). The observation of a slight temperature rise of the resistivity of the uncleaved single crystals along *ab* plane and semiconducting behavior along *c* axis is supporting this interpretation.

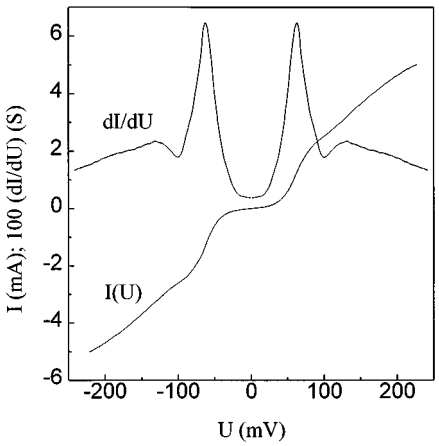

FIG. 8. Current-voltage and conductance-voltage characteristics of $Bi_2Sr_2CaCu_2O_{8+x}$ ($T_C = 83$ K) break junctions at $T = 4.2$ K.

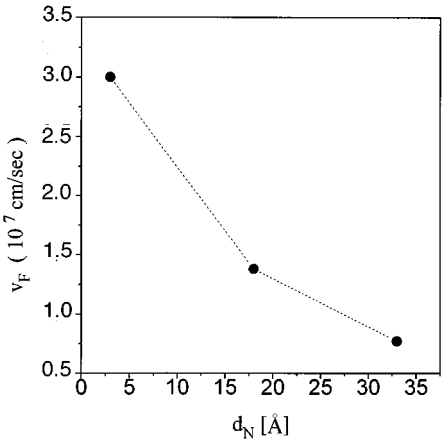

FIG. 9. Variation of the Fermi velocity with the thickness of the *N* layer, as deduced from the data in Table I and Fig. 6.

The fit parameters did not allow us to extract the thickness of or the Fermi velocity in the *N* layer, since only the ratio of these enters the fitting parameter *R*. Using the proposed interpretation for the discreteness of E_1 values, the thickness d_N can be defined. Assuming the formation of the symmetric SN_1IN_2S contacts, three characteristic E_1 values can be explained in the histogram in Fig. 6. Peak *A* with energy $2 \times E_{1A} = 58$ meV corresponds to the contact with geometry *S*/3 Å/*I*/3 Å/*S*, when only one peak at $E \approx 2\Delta_S$ present on the conductance-voltage characteristic (Fig. 5). Peak *B* corresponds with energy $2 \times E_{1B} = 48$ meV to the *S*/18 Å/*I*/18 Å/*S* (Fig. 4). Peak *C* corresponds with energy $2 \times E_{1C} = 20$ meV to the *S*/33 Å/*I*/33 Å/*S*. These types of contacts show the largest number of peaks (Fig. 3). Since, in a real situation the formation of asymmetric *S*-*N*-*I*-*N*-*S* contacts cannot be excluded, additional E_1 values can occur. Hence, peak *D* should correspond with energy $E_{1A} + E_{1B} = 53$ meV to the contact *S*/3 Å/*I*/18 Å/*S*, peak *E* with energy $E_{1A} + E_{1C} = 39$ meV to the *S*/3 Å/*I*/33 Å/*S*, and peak *F* with energy $E_{1B} + E_{1C} = 34$ meV to the *S*/18 Å/*I*/33 Å/*S*.

The peak in E_1 values at 70 meV, representing about 10% of all data, cannot be explained by considered above procedure. Rather, it is related to the contacts with tunneling current within the *ab* plane. Figure 8 shows the example of $I(U)$ and $dI(U)/dU$ characteristics with an energy gap of about $2\Delta_{ab} = 70$ meV, which are typical for *ab*-plane tunneling.[28–30]

Assuming a *c*-axis-oriented *S*-*N*-*I*-*N*-*S* contact geometry yielding discrete d_N values, the Fermi velocity can be deduced from the data (Table I). As shown in Fig. 9, Fermi velocity increases with decreasing d_N. By simple approximation to the limit $d_N \rightarrow 0$, the Fermi velocity in the CuO plane along the *c* axis can be estimated to be $v_F \approx 3.3 \times 10^7$ cm/s. This value is in remarkable agreement with the expected value $v_F \approx 3 \times 10^7$ cm/s, as it was calculated for YBaCuO superconductor.[31] It should be noted that, corre-

sponding to our data the anisotropy of the energy gap in CuO planes is not essential $\eta=\Delta_{ab}/\Delta_c\approx 35/29\approx 1.2$.

CONCLUSIONS

A broad variation of tunneling spectra has been found in BiSrCaCuO single-crystal break junctions. In particular, a periodic structure has been observed in the conductance-voltage characteristics. This behavior was explained by assuming of the formation of a proximity N layer at the surface. Electron-hole interferences in the N layer produce the oscillations in the tunneling DOS, which, in turn, lead to current steps in the $I(U)$ and peaks in the $dI(U)/dU$ characteristics. It is important to note that the presence of a sharp energy gap in the S layer is an important condition for the interference effect.

Using Arnold's proximity model in the clean limit, the Fermi velocity in Bi-Sr-Ca-Cu-O has been evaluated. A small anisotropy of the energy gap in the CuO layers has been found with $2\Delta_{ab}/kT_c\approx 9.8$ ($\Delta_{ab}\approx 35$ meV) and $2\Delta_c/kT_c\approx 8.1$ ($\Delta_c\approx 29$ meV).

The presented data are important for the explanation of the reported discrepancy of energy-gap values for Bi-Sr-Ca-Cu-O. It is important to note that the peak in the conductance-voltage characteristics is in many cases not related to the energy gap, but to a bound state.

As mentioned before, the existence of bound states has been demonstrated on artificial S/N-I-S (Pb/Zn-I-Pb) sandwiches with thick 2–5 μm normal layers.[12] It is remarkable that in our measurements bound levels were observed with break-junction contacts between two cryogenically cleaved fractures, where the interference effect takes place in the electrode surface itself and on an essentially smaller thickness scale.

ACKNOWLEDGMENTS

The authors are indebted to A. Golubov and M. Yu. Kupriyanov for stimulating discussions. This work was supported in part by German DFG under Contract No. MU 710/2-1.

[1] W. L. McMillan and J. M. Rowell, *Superconductivity*, edited by R. D. Parks (Marcel Dekker, New York, 1969).
[2] J. R. Kirtley, Int. J. Mod. Phys. B **4**, 201 (1990).
[3] G. Deutscher and K. A. Müller, Phys. Rev. Lett. **59**, 1745 (1987).
[4] B. A. Aminov, L. Roshta, Ya. G. Ponomarev, and M. V. Sudakova, Sov. J. Low Temp. Phys. **17**, 363 (1990).
[5] A. Chang, Z. Y. Rong, Yu. M. Ivanchenko, T. Luand, and E. L. Wolf, Phys. Rev. B **46**, 5692 (1992).
[6] W. L. McMillan, Phys. Rev. B **175**, 537 (1968).
[7] W. L. McMillan, Phys. Rev. B **175**, 559 (1968).
[8] G. B. Arnold, Phys. Rev. B **18**, 1076 (1978); **23**, 1171 (1981).
[9] M. Boekholt, Th. Bollmeier, L. Buschmann, M. Fleuster, and G. Güntherodt, Physica C **198**, 33 (1992).
[10] J. E. Zimmerman *et al.*, J. Appl. Phys. **41**, 1572 (1970); J. Moreland and J. W. Ekin, *ibid.* **58**, 3888 (1985).
[11] P. J. M. van Bentum, R. T. M. Smokers, and H. van Kempen, Phys. Rev. Lett. **60**, 2543 (1988); P. Wilkins, M. Amman, R. E. Soltis, E. Ben-Jacob, and R. C. Jaklevich, Phys. Rev. B **41**, 8904 (1990); E. J. Boon, A. J. A. van Roy, and H. van Kempen, Physica C **235-240**, 1879 (1994).
[12] K. K. Likharev, IBM J. Res. Dev. **33**, 144 (1988).
[13] D. Bellanger, J. Klein, A. Leger, M. Belin, and D. Defournean, Phys. Lett. A **42**, 459 (1973).
[14] J. M. Rowell, Phys. Rev. Lett. **30**, 167 (1973).
[15] P. G. de Gennes and D. Saint-James, Phys. Lett. **4**, 151 (1963).
[16] J. M. Rowell and W. L. McMillan, Phys. Rev. Lett. **16**, 453 (1966).
[17] M. Tanaka *et al.*, Nature (London) **339**, 691 (1989).
[18] Z. Zhang and Ch. M. Leider, Phys. Rev. B **46**, 5845 (1992).
[19] T. Hasegawa, M. Nantoh, H. Ikuta, and K. Kitazawa, Physica C **185-189**, 1743 (1991).
[20] B. A. Aminov *et al.*, Physica C **224**, 321 (1994).
[21] V. Z. Kresin and S. A. Wolf, Phys. Rev. B **46**, 6458 (1992).
[22] M. Tachiki and S. Takahaschi, Physica C **191**, 363 (1992).
[23] C. Hu, Phys. Rev. Lett. **72**, 1526 (1994); J. H. Xu, J. H. Miller, Jr., and C. S. Ting, Phys. Rev. B **53**, 3604 (1996); S. Kashiwaya, Y. Tanaka, M. Koyanagi, and K. Kajimura, *ibid.* **53**, 2667 (1996).
[24] A. I. Buzdin, V. P. Damjanovic, and A. Yu. Simonov, Physica C **194**, 109 (1992).
[25] A. A. Abrikosov and R. A. Klemm, Physica C **191**, 224 (1992).
[26] S. H. Liu and R. A. Klemm, Phys. Rev. B **52**, 9657 (1995).
[27] B. T. Stojkovic and O. T. Valles, Phys. Rev. B **50**, 3374 (1994).
[28] D. Mandrus, L. Forro, D. Koller, and L. Mihaly, Nature (London) **351**, 460 (1991).
[29] J. W. Kawe, Q. Chen, and K.-W. Ng, Physica C **235-240**, 1877 (1994).
[30] J. J. Wnuk *et al.*, Supercond. Sci. Technol. **4**, S412 (1991).
[31] P. B. Allen, W. E. Pickett, and H. Krakauer, Phys. Rev. B **37**, 7482 (1988).